Hybrid optical antenna with high directivity gain

Alireza Bonakdar and Hooman Mohseni*

Bio-inspired Sensors and Optoelectronics Laboratory (BISOL), Department of Electrical Engineering and Computer Science, Northwestern University, Evanston, Illinois 60208, USA

**Corresponding author: hmohseni@northwestern.edu*

Received March 26, 2013; revised June 6, 2013; accepted June 26, 2013; posted July 1, 2013 (Doc. ID 187526); published July 24, 2013

Coupling of a far-field optical mode to electronic states of a quantum absorber or emitter is a crucial process in many applications, including infrared sensors, single molecule spectroscopy, and quantum metrology. In particular, achieving high quantum efficiency for a system with a deep subwavelength quantum absorber/emitter has remained desirable. In this Letter, a hybrid optical antenna based on coupling of a photonic nanojet to a metallo-dielectric antenna is proposed, which allows such efficient coupling. A quantum efficiency of about 50% is predicted for a semiconductor with volume of $\sim\lambda^3/170$. Despite the weak optical absorption coefficient of 2000 cm^{-1} in the long infrared wavelength of ~8 μm, very strong far-field coupling has been achieved, as evidenced by an axial directivity gain of 16 dB, which is only 3 dB below of theoretical limit. Unlike the common phased array antenna, this structure does not require coherent sources to achieve a high directivity. The quantum efficiency and directivity gain are more than an order of magnitude higher than existing metallic, dielectric, or metallo-dielectric optical antenna.

OCIS codes: (040.0040) Detectors; (040.5160) Photodetectors; (040.5570) Quantum detectors; (040.6070) Solid state detectors; (080.3630) Lenses; (110.3080) Infrared imaging.

http://dx.doi.org/10.1364/OL.38.002726

Coupling between electronic state and far-field light in optical processes such as absorption and spontaneous emission is a central issue for applications such as quantum metrology [1], optical quantum information [2], single molecule fluorescence spectroscopy [3], and ultrasensitive detection [4,5], which demand high quantum efficiency. In such applications, propagating far-field light with diffraction limited spatial distribution has to be coupled to the electronic state of a quantum absorber/emitter with the scale far below the diffraction limit. A straightforward solution is to convert far-field optical modes to near-field modes with a dimensional scale closer to the electronic state. The process of converting far-field to near-field and vice versa can be achieved by an antenna as an intermediate element between far-field mode and electronic state in a quantum element (absorber/emitter).

Here, we propose a hybrid antenna, which has a high directivity and very low loss, leading to a large antenna directivity gain. In order to analyze the advantages of the proposed antenna, we follow a similar approach as [6], to describe energy transfer steps involved in such coupling.

Antenna performance is characterized by a set of figures of merit. In the following definitions, we assume an antenna is coupling far-field to a quantum load. Antenna efficiency is defined as the ratio of the power delivered to load P_L to the total power P_T received by the antenna from far-field:

$$\eta = \frac{P_L}{P_T} = \frac{P_L}{P_L + P_{\mathrm{Loss}}}, \tag{1}$$

where P_{Loss} is the dissipated power, which is stored/wasted/scattered by the antenna. Usually an antenna has a limited range of responsivity to the far-field's spatial distribution and direction beyond which it cannot capture light efficiently. In order to quantify the antenna tolerance to its far-field profile, one can define directivity

$$D(\theta,\varphi) = \frac{4\pi}{\iint P_L(\theta,\varphi)\mathrm{d}\theta\mathrm{d}\varphi} P_L(\theta,\varphi), \tag{2}$$

where $P_L(\theta,\varphi)$ is the power captured by load when the antenna is excited by a planewave with the wave vector in the direction of (θ,φ). The antenna gain determines the efficiency (η) of coupling between far-field optical mode with a specific direction to the load:

$$G(\theta,\varphi) = \eta D(\theta,\varphi). \tag{3}$$

Aside from the antenna's interaction with quantum source/load, the antenna interaction with far-field zone can also affect the overall performance. The dimension of the antenna can set an inherent limit on the antenna response to far-field. In fact, the upper limit of antenna gain is derived as [7]

$$G_{\max} = (ka)^2 + 2ka, \tag{4}$$

where k is the optical wave vector incident on antenna and a is the radius of the smallest possible hypothetical sphere that encloses the antenna. As is evident in this equation, miniaturization of antenna can deteriorate antenna performance: by shrinking antenna size, $G_{\max}$ decreases, which can be attributed to the fact that the antenna becomes less efficient in radiating power to far-field due to coupling of optical modes to the antenna's nonradiative high-order modes [8]. Based on reciprocity, we can adapt the limitation for the case of antenna receiving power from far-field and delivering to the quantum load: by reducing antenna size, the total amount of power captured by antenna will reduce, which directly reduces the power delivers to load, resulting in lower $G_{\max}$.

We now propose an example of a hybrid antenna that delivers power to a deep subwavelength semiconductor absorbing volume effectively. The hybrid antenna is composed of a dielectric antenna, and a metallo-dielectric antenna. The former efficiently couples optical power from far-field to the latter, which in turn couples the power to the semiconductor absorbing volume. The dielectric antenna is a lossless dielectric microsphere with diameter 20 μm and refractive index ~1.5, which can focus far-field wavelength λ into a photonic jet—a narrow, intensive, propagative beam with a beamwidth of $\sim\lambda/3$ and depth $\sim\lambda$ [9–11]. Unlike a conventional microlens focused beam to which the width (W) and depth (Z) of the focused beam is related by Rayleigh range, $Z = \pi W^2/(2\lambda)$ [12], the photonic jet's width and depth do not follow the Gaussian profile and depth is at least twice the predicted Rayleigh length. In the following, we show that the photonic nanojet produces much superior coupling compared with a Gaussian beam. The metallo-dielectric antenna forms a cavity that encloses an absorptive region (interband or intersubband) having dimensions 1.5 μm × 2 μm × 1 μm and a weak absorption coefficient. Here we assumed a typical value of absorption coefficient of 2000 cm^{-1} at the operating wavelength $\lambda \sim 8$ μm [13]. Recently, such metallo-dielectric cavity is utilized to make nano-lasers [14].

The proposed structure is shown in Fig. 1. A 50 nm thin oxide layer with refractive index ~1.5 is placed to separate the cavity into top and back contacts of the detector (made of gold) to prevent a short circuit. The experimental value is considered for the dielectric function of gold. We used FDTD to simulate the response of the hybrid antenna to a Gaussian optical source with 24 μm beamwidth and linear polarization along x direction. The Gaussian beam is illuminating the device from the bottom of the microsphere antenna. All boundary conditions are assumed to be a perfectly matched layer. The metallo-dielectric cavity with the subdiffraction dimensions couples the focused photonic nanojet efficiently to the tightly cavity mode. Light confinement at the cavity can increase light absorption in the semiconductor significantly. Unlike devices based on conventional optics, the hybrid antenna allows shrinking the device volume beyond the diffraction limit to reduce dark current without large degradation of QE [4]. Despite optical absorption enhancement, this metallo-dielectric cavity cannot

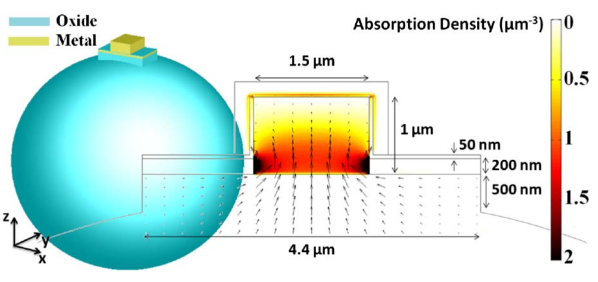

Fig. 1. Schematic of the hybrid antenna (left) and cross sectional view of the microcavity part at $y = 0$ plane (right). The origin of the coordinate coincides with the center of the microsphere. The cross section view is superimposed by the map of power flow (arrows of Poynting vectors scaled with their relative local strength) and normalized power consumption density (optical absorption density) throughout the cavity at the operating wavelength $\lambda \sim 8$ μm. Despite the deep subdiffraction volume of $\lambda^3/170$, the photonic nanojet power can efficiently reach into the cavity. The integral of the absorption density over the absorbing region gives the overall QE.

capture far-field power efficiently without microsphere antenna due to its limited dimensions in the real space. Increasing the dimensions cannot improve QE due to elevation of ohmic loss in metallic components. Figure 1 also shows the map of Poynting vector flow at the vertical cross section of the structure. The background color map is the optical absorption density in the cavity, which is the ratio of the divergence of Poynting vector (dropping its negative sign due to lossy medium) to the source power. The integral of the absorption density over the absorbing region gives QE.

The power flow demonstrates how the photonic nanojet is converted into cavity mode and harvested by semiconductor at the cavity. The power spectrum that is absorbed by the active region and dissipated in the metallic components is calculated and plotted in Fig. 2 as a function of cavity height. The peaks of QE are corresponding to distinguished cavity modes as specified in Figs. 2(a)–2(c). The first-order cavity mode at optical wavelength around 8 μm can be harvested by the active region with near 50% efficiently, while the volume of absorptive region is as small as $\lambda^3/170$. Thus, the optical antenna strongly couples the Gaussian mode to the active region with deep subdiffraction size.

In order to evaluate the impact of the microsphere antenna and metallo-dielectric cavity on the QE, we simulate structures in the absence of either the cavity (removing metallic components) or the dielectric microsphere, and compare the results as shown in Fig. 3(a) using the optimized geometrical specifications of the first-order mode at 8 μm optical wavelength. QE of hybrid antenna is at least one-order of magnitude larger compared with the cases without either cavity or microsphere and almost three-orders of magnitude larger compared with a freestanding slab of semiconductor absorber with the same dimension as inside the cavity. The photonic nanojet produced by the microsphere

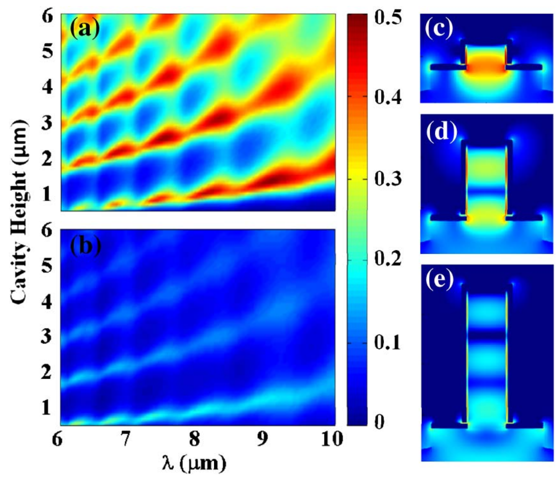

Fig. 2. Normalized optical power spectrums (a) harvested by semiconductor absorber (QE) and (b) dissipated in metal versus different cavity heights. Hybrid antenna elevates QE to approximately 50% with moderate level of metal loss (less than 18%) at $\lambda \sim 8$ μm. (c) Electric field intensity profile of the cavity mode (log-scale) at $\lambda \sim 8$ μm with cavity height of 1 μm (first-order mode), (d) 3 μm (second-order mode), and (e) 5 μm (third-order mode). The field intensity is scaled from zero to unity.

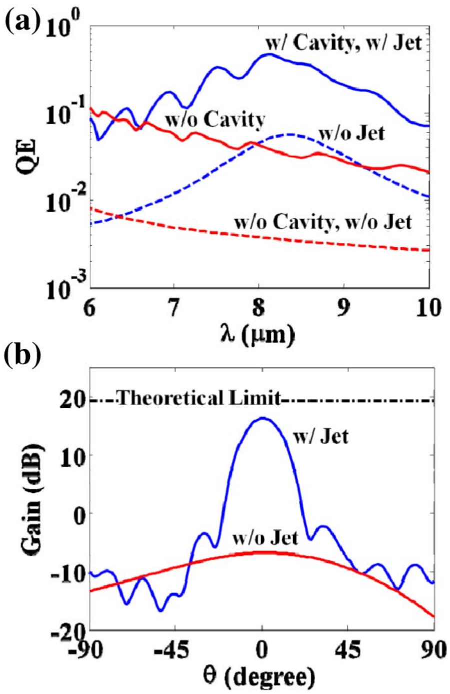

Fig. 3. (a) Effect of metallo-dielectric cavity and photonic nanojet on QE. The hybrid optical antenna has superior performance in terms of QE over the other conventional structures evaluated here. (b) Comparing directivity gain of antenna with and without microsphere antenna. Microsphere dielectric can enhance directivity gain near 22 dB (150 times) and to reach 3 dB below the theoretical limit.

antenna has significantly better coupling efficiency to cavity modes, compared with Gaussian beams produced from microlenses. For example, a conventional microlens with similar diameter [15] produces a five-times weaker coupling. Similarly, antireflection coating can reduce the reflection, but the lack of efficient coupling to cavity results in about two-orders of magnitude lower QE.

The directive gain of the antenna at 8 μm optical wavelength as a function of θ is simulated. Then, far-field is calculated and is used in Eqs. (2) and (3) to calculate the directivity gain. Figure 3(b) compares the directivity gain of the metallo-dielectric antenna with and without microsphere antenna. The photonic nanojet, produced by the microsphere, improves directivity gain as much as 22 dB. The gain is very close to the fundamental limit of ~20 dB. Such a high directivity can suppress off-axis blackbody radiation and reduce noise. The axial profile of directivity gain as a result of microsphere incorporation indicates its contribution to enhance the antenna gain without adding loss to the system. Higher values of directivity gain could be achieved by larger microsphere without significant reduction of QE due to nonresonance and lossless nature of photonic nanojet. The asymmetric results of far-field in Fig. 3(b) come from the randomness of dipole sources used in numerical modeling.

In conclusion, we presented a hybrid antenna that overcomes poor directivity gain due to deep subdiffraction dimensions of conventional metallic optical antennas. The load of the hybrid antenna can absorb nearly 50% of the incident optical power from far-field, despite its weak optical absorption coefficient of 2000 cm^{-1} and deep subwavelength volume $\sim\lambda^3/170$ at infrared wavelength of ~8 μm. Moreover, directivity gain was 16 dB, which is only 3 dB below the theoretical limit. The presented antenna configuration could lead to efficient energy harvesting, as well as photon detecting processes.

This work was supported in part by the NSF (grant no. EECS-1206155), ARO (grant nos. W911NF-1-0390, W911-NF-12-1-0324), and high performance computational center (QUEST) at Northwestern University.

References

1. S. V. Polyakov and A. L. Migdall, J. Mod. Opt. **56**, 1045 (2009).
2. R. H. Hadfield, Nat. Photonics **3**, 696 (2009).
3. O. L. Muskens, V. Giannini, J. A. Sánchez-Gil, and J. Gómez Rivas, Nano Lett. **7**, 2871 (2007).
4. A. Bonakdar and H. Mohseni, Infrared Physics & Technology **59**, 142 (2013).
5. W. Wu, A. Bonakdar, and H. Mohseni, Appl. Phys. Lett. **96**, 161107 (2010).
6. L. Novotny and N. van Hulst, Nat. Photonics **5**, 83 (2011).
7. R. F. Harrington, J. Res. Natl. Bur. Stand. **64**, 1 (1960).
8. M. Agio, Nanoscale **4**, 692 (2012).
9. A. Heifetz, S.-C. Kong, A. V. Sahakian, A. Taflove, and V. Backman, J. Comput. Theor. Nanosci. **6**, 1979 (2009).
10. W. Wu, D. Dey, O. G. Memis, A. Katsnelson, and H. Mohseni, Nano. Res. Lett. **3**, 123 (2008).
11. W. Wu, D. Dey, O. Memis, A. Katsnelson, and H. Mohseni, Nano. Res. Lett. **3**, 351 (2008).
12. J. N. Damask, *Polarization Optics in Telecommunications* (Verlag, 2004), Vol. **101**.
13. A. Rogalski, Prog. Quantum Electron. **27**, 59 (2003).
14. M. P. Nezhad, A. Simic, O. Bondarenko, B. Slutsky, A. Mizrahi, L. Feng, V. Lomakin, and Y. Fainman, Nat. Photonics **4**, 395 (2010).
15. J. Y. Kim, N. B. Brauer, V. Fakhfouri, D. L. Boiko, E. Charbon, G. Grutzner, and J. Brugger, Opt. Mater. Express **1**, 259 (2011).